Chapter

Laser Treatment CVD Diamond Coated Punch for Ultra-Fine Piercing of Metallic Sheets

Tatsuhiko Aizawa, Tadahiko Inonara, Tomoaki Yoshino, Tomomi Shiratori and Yohei Suzuki

Abstract

CVD-diamond coated special tools have been widely utilized to prolong their tool life in practical production lines. WC (Co) punch for fine piercing of metallic sheets required for high wear-toughness to be free from chipping and damages and for high product quality to punch out the holes with sufficient dimensional accuracy. The laser trimming process was developed to reduce the surface roughness of diamond coating down to submicron level and to adjust its diamond layer dimensions with a sharp punch edge for accurate piercing. The pulsed laser irradiation was employed to demonstrate that micro-groove was accurately formed into the diamond coating. Less deterioration in the worked diamond film by this laser treatment was proved by the Raman spectroscopy. The femtosecond laser trimming was proposed to sharpen the punch edge down to 2 μm and to form the nano-textured punch side surfaces with the LIPSS (Laser Induced Periodic Surface Structuring)-period of 300 nm. Fine piercing experiments were performed to demonstrate that punch life was significantly extended to continuous punching in more than 10,000 shots and that mirror-shining hole surfaces were attained in every shot by regularly coining the nanotextures. The sharp punch edge with homogeneous edge profile was responsible for reduction of the induced damages into work sheet by piercing. The punch life was extended by the ejection mechanism of debris particles through the nanotextures on the punch side surface. The present laser treatment was useful in trimming and nanostructuring the complex-shaped punch edge for industrial application.

Keywords: CVD diamond coated WC (Co) tools, laser adjustment, laser trimming, punch edge sharpening, punch nano-structuring, ultrafine piercing, AISI316L sheets, debris particle ejection

1. Introduction

The CVD (Chemical Vapor Deposition)-diamond coating as well as the PCD (Poly-Crystalline Diamond)-chip have been widely utilized as a protective layer of special tools to prolong their life [1]. In addition to their application to cutting tools, the sintered diamond dies were employed as a tool in the metal forming [2]. In particular, the CVD-diamond coated tools become a standard procedure to cut the CFRP (Carbon Fiber reinforced plastic) members [3], to make deep drawing of

stainless steel sheets to cups [4] and to precisely punch out the high strength copper alloy plates [5]. During those manufacturing processes, the diamond coating is usually damaged and chipped so that the tool substrates have to be recycled by removing away or ashing the used coatings before being wasted as an industrial dust.

Let us remember that WC (Co) and silicon were only utilized as a substrate for hot-filament CVD processes to have thick, uniform diamond layer. In particular, the cobalt content in WC (Co) substrate is optimally selected for proper nucleation and growth of diamond coating in practice. In order to improve the material efficiency in the coming circular economy, these used DLC- and diamond-coated cutting tools and forming dies must be recycled to reuse the original WC (Co) substrate for higher cost-competitiveness. In this circulation of WC (Co) substrates [6], the perfect removal or ashing of diamond film and metallic buffer layers with minimum damage to tool geometry is an essential process to reuse the WC (Co) as illustrated in **Figure 1**. RF (Radio-Frequency) – DC (Direct Current) plasma ashing process was developed to make perfect removal of the used DLC coatings without significant damages to substrates and to reuse the as-ashed WC (Co) substrate for recoating [7–12]. As pointed in [13], the oxygen ion density in those ashing processes must be intensified enough to remove the used CVD-diamond coating with sufficiently high removal rate. This high density plasma ashing method has proper capacity to remove the diamond films even on the rake surfaces of cutting tool blades with less blade edge loss than 1 μm [14–16]. Hence, as a challenging issue in **Figure 1** for circulation economy of WC (Co) tool substrates, the CVD-diamond coated tools must be shaped to have high capability for cutting and shearing in practical operations and to improve the total WC (Co) efficiency.

As-coated diamond film has a rough surface due to its three dimensional crystalline growth; the maximum surface roughness must be reduced down to the tolerance in the industrial applications, less than 0.5 μm. Its geometrical profile is never adaptive to the precise stamping tools; its surfaces must be trimmed to have accurate dimensions as a tool for fine cutting, shearing and piercing within the deviation of 1 μm. In addition, the diamond-coated tools and dies must have sharp edges enough to preserve the highly burnished surfaces of products. Furthermore, their lives must be elongated by reducing the adhesion of work material debris.

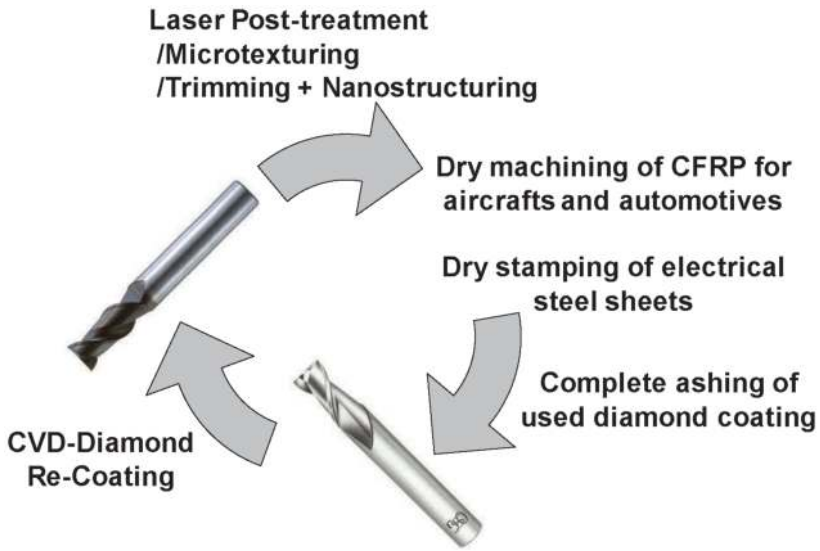

Figure 1.
A circular economy of WC (Co) tools by the precise treatments of diamond coatings.

In the present chapter, among the laser processings [17, 18], the laser treatment of CVD-diamond coated tools is proposed to geometrically adjust their diamond coating profile, to trim their surfaces and sharpen their edges and to form the nanostructured micro-grooves for in situ ejection of debris particles during piercing process. Since the first world-wide notice on the importance of wear debris [19], a role of debris particles on the tribological performance in metal forming has been studied both in academic and industries. In particular, fine debris fragments induced the fretting wear in metal forming; how to eject those debris particles still becomes an issue of nuisance [20]. Hence, this laser nanostructuring technique is a powerful approach to prolong the fine piercing punch life and to control the piercing process for both ductile and brittle work sheets.

Furthermore, this laser nanostructuring provides a method to design and fabricate the engineered surfaces to mechanical elements such as the channel, the orifice and the heat sink. If their inner and outer surfaces have an appropriate nanostructure, these structured surfaces are expected to work as an engineered surface with higher wettability, more hydrophobicity and larger overall heat penetration. In the case of the orifice, the leak flow of gasoline through the orifice walls is minimized by their hydrophobicity of nanotextured surface [21, 22]. A nanotextured heat sink has a capacity to significantly improve the heat transfer coefficient, especially the boiling water heat transfer capacity [23, 24]. In particular, the AISI316L orifice plate is a target for the present fine piercing by the nanostructured surface to improve its surface property control.

A CVD-diamond coated WC (Co) specimen is first employed to demonstrate that the pulsed laser adjustment is effective to shape the diamond coated tools and to make microtexturing to diamond films without significant damage to the diamond structure. Next, the femtosecond laser micro-machining is employed to trim a diamond-coated piercing punch. This laser trimming enables to reduce the roughness of as-coated diamond films and to sharpen the punch edge width down to 2 μm. Furthermore, the nanotextures with the period of 300 nm are formed from the edge to the specified length on the punch side surfaces, simultaneously with trimming. Finally, the micro-stamping system is utilized to describe the piercing behavior of AISI316L austenitic stainless steel and amorphous steel sheets with the use of this laser trimmed punch. When using the WC (Co) punch with the sharpened edge, its piercing of AISI316L sheets partially induced a fractured hole surface; the burnished surface area ratio was limited by 70 to 80% of their whole pierced hole surface [25]. In addition to fine piercing performance with full burnished area ratio, the nanotextures on the punch side surface is concurrently transcribed onto the AISI316L holes together with this trimming. Due to this imprinting of the laser-trimmed punch surface with nanostructures, a mirror-shining hole surface is fabricated also to have a periodic nanotexture. An amorphous electrical steel sheet is also employed to investigate the piercing performance of brittle work materials [26]. The sharp edge profile and the nanostructured punch side surface have influence to reduce the damaged width and to improve the product quality. SEM (Scanning Electron Microscopy) and WIS (White Interference Spectroscopy) analyses are utilized to describe this formation of nanostructures into diamond-coated punch and their duplication onto the product surface.

2. Laser treatment of CVD-diamond coated tools

Two types of laser treatment system are proposed to make geometric adjustment of CVD diamond coated punch with the use of pulsed laser irradiation and to trim the punch edge and make nanostructuring onto the side surface

of punch with the use of femtosecond lasers. These two laser treatments are illustrated in **Figure 2**.

2.1 Geometric adjustment by excimer laser irradiation

As-CVD-coated diamond film with the thickness of 20 μm has a surface roughness of 3 to 5 μm. A sizing treatment [27, 28] process is necessary to reduce the surface roughness within tolerance for tooling in metal forming and to fit the surface profile of punch into tailored geometry for fine piercing and embossing. The pulsed laser irradiation process is employed to remove the unnecessary surface parts of CVD-diamond film through a series of shots in order that the whole surface profile should be fine enough to satisfy the designed CAD (Computer Aided Design) data of tools.

Figure 2a illustrates an experimental set-up for this sizing treatment. As-coated punch was fixed into a jig, which was located on the X-Y stage. With the use of this stage and Z-positioning controller, the work area on the punch surface was located

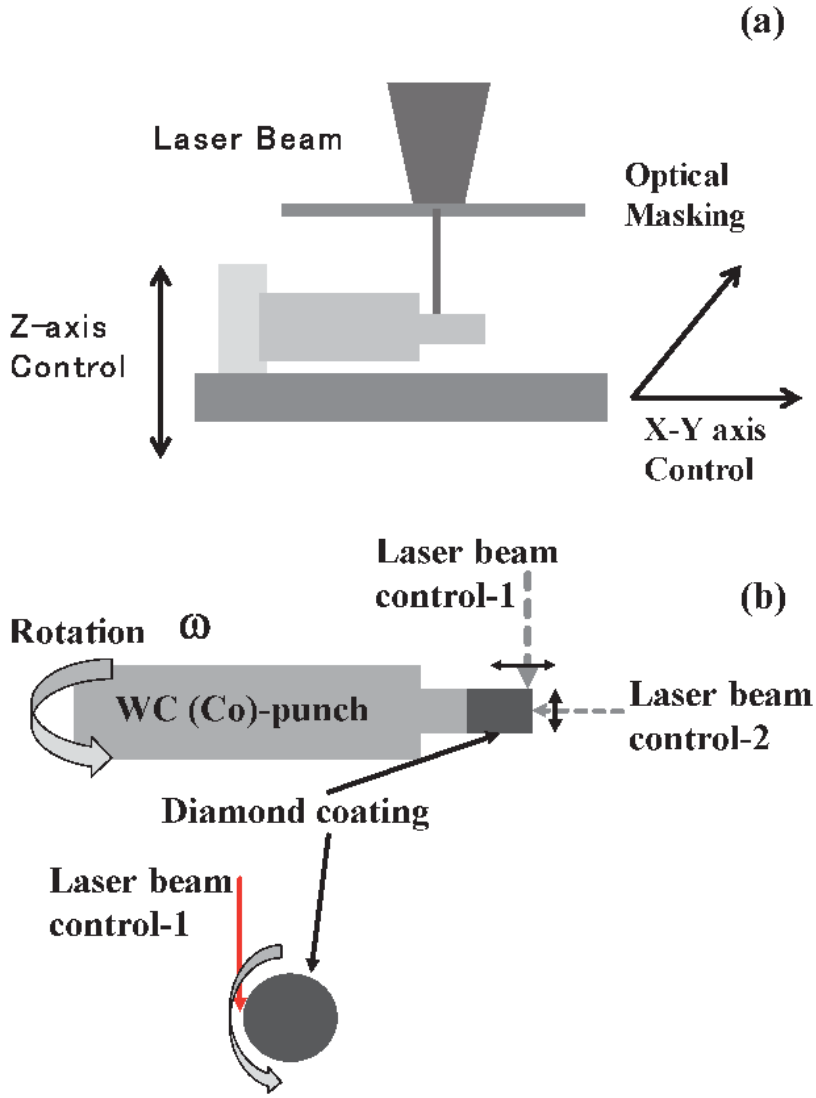

Figure 2.
Two types of laser treatments for the diamond coated tools for fine and ultrafine piercing. (a) Geometric adjustment by pulsed laser irradiation, and (b) trimming by femtosecond laser machining.

for laser irradiation. After the pulsed irradiation, this work area was relocated for next irradiation. The number of pulses was directly controlled to correspond to each feeding depth for removal of diamond coating. A laser spot area was also controlled by optical masking; e.g., one segment on the mask became a transparent window for the pulsed laser beam to irradiate this segmented surface area of work. In this process, the removed thickness of CVD coating by single shot via laser abrasion was optimally determined to be around 0.1 μm by controlling the power profile of laser beams. The original laser beam was modified by the optical masking technique to focus only onto the segment of 250 μm x 125 μm. In the following experiments, the diamond coated punch was controlled to move stepwise in the X axis by 250 μm to form a rectangular micro-groove onto the diamond coating with the width of 125 μm.

2.2 Trimming and nanotexturing by femtosecond laser irradiation

The femtosecond laser micromachining is suitable to trimming and nanotexturing the CVD-diamond coated WC (Co) punches [29–31] for ultrafine piercing of metallic sheets [29–32]. **Figure 2b** depicts the standard setup for this laser trimming and nanotexturing. The side surface was first trimmed by utilizing the laser beam control-1. The punch head was secondly processed by using the control-2. The laser beam was moved from the center to the end of the punch head. The fluence was also held constant at 0.265 J/cm^2. During this two-step procedure in the experiment, the end of the punch was held in a jig to be rotated with a constant velocity by ω = 7.2 degrees/s. The galvanometer was utilized to distribute the laser beam as tailored by CAM (Computer Aided Machining) data for the trimming operation. The capacity of present femtosecond laser machining system is stated in the following. The wavelength of the femtosecond laser was 515 nm, the pulse width was 200 fs, and the pulse repetition rate was 400 kHz. The maximum average power was 40 W, and the maximum pulse energy was 50 μJ. The working stage was 300 mm × 300 mm. A work material with sized 280 mm × 150 mm was placed on the X- and Y-axes controlled stage in **Figure 2b**. The single-shot power was estimated to be 0.25 GW. High-powered irradiation of 200 fs was used to drive the well-defined ablation into the targeted materials.

The laser nanostructuring method stands on the LIPSS (Laser Induced Periodic Surface Structuring) performance [33, 34]. The directional nanotexture was in situ formed together with the laser trimming during the femtosecond laser machining process with a skew angle against the beam scanning direction. In the following experiments, the fluence was constant with 0.6 J/cm^2. The laser machining track overlapped the working range 20 times by rotating the work. The LIPSS-ripple period was controllable by the laser fluence, pulse width, and so forth for femtosecond laser nanotexturing. In fact, LIPSS using high and low spatial frequencies with very different periods can be produced via the same laser setup, depending on the process conditions. This LIPSS-ripple period was estimated to be 250 nm in the present trimming conditions. To be discussed later, this LIPSS period as well as the nanostructuring alignment are controllable by the laser processing conditions during the optical polarization and transformation processes.

3. Micro-grooving of diamond-coated tools by pulsed laser irradiation

An excimer laser machining system (LIPS-Works, Co., Ltd.) was employed to make pulse laser irradiation of CVD-diamond coated rectangular punch. A micro-groove was formed onto the diamond coating to describe the dimensional accuracy

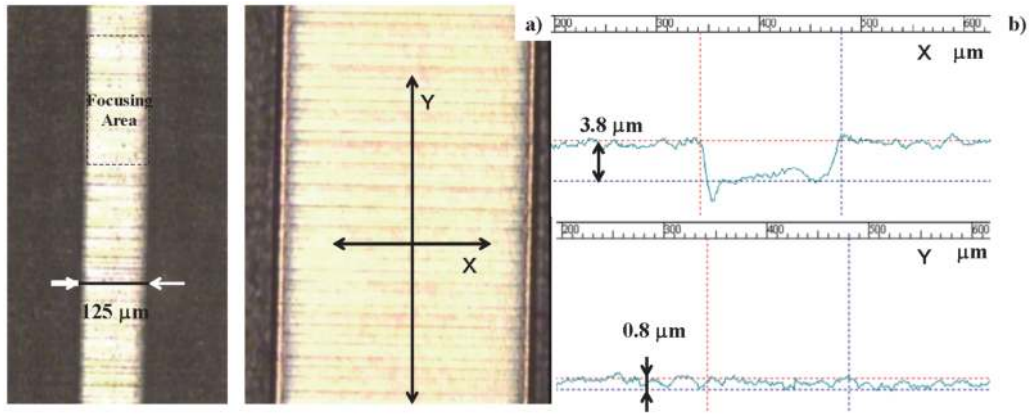

Figure 3.
Micro-grooved diamond coating by the pulsed laser machining. (a) a micro-groove with the width of 125 mm with low and high magnifications, and (b) its surface depth profiles along the X- and Y-axes.

in sizing treatment of diamond coated punch. Raman spectroscopy was employed to characterize the diamond film before and after this micro-grooving process.

3.1 Micro-grooving of diamond-coated tool substrate

The excimer laser was employed to make micro-grooving onto the CVD-diamond coating. In each pulsed laser irradiation, the area of 250 μm x 125 μm x 0.1 μm was stepwise removed by a single shot. After multi-shot irradiation, the punch was relocated to move in the X axis by 250 μm to continue this laser ablation process till the end of punch width. The number of laser pulse shots is constant by 50.

Figure 3a depicts the laser-machined track of CVD-diamond coating. Without damages to the un-irradiated surface, only a single micro-groove with the width of 125 μm is accurately cut-in by the present laser machining. This linear removal of coating takes place only with positioning control of specimens without any change in the laser irradiation conditions. The feeding depth is controlled by the number of shots independently from the above spatial control. This results in precise profiling of CVD-coated tool surface geometry in the suitable manner to tooling design. The laser-microscope (Laser-tech, SD 100; Tokyo, Japan) was utilized to measure the surface roughness distributions both in the longitudinal and the lateral directions of linear track. **Figure 3b** depicts the micro-groove surface depth profiles in the X- and Y-axes, respectively. Its average depth is 3.8 μm, and a deep valley is seen at either edge of micro-groove. This might be because the laser energy profile is intensified at the edge of masking window. The maximum roughness in the longitudinal direction at the bottom of micro-groove is only 0.8 μm. This proves that this sizing process by pulsed laser irradiation accurately adjusts the punch edge profile as demanded by the engineering CAD.

4. Raman spectroscopy on the laser treatment effect on diamond

Raman spectroscopy (Renishaw, Co., Ltd.) was utilized to characterize the effect of the laser adjustment to the microstructure of CVD diamond. **Figure 4** compares the Raman spectra and their deconvoluted profiles before and after laser adjustment. As-coated diamond is characterized by the graphite disordered D peak at

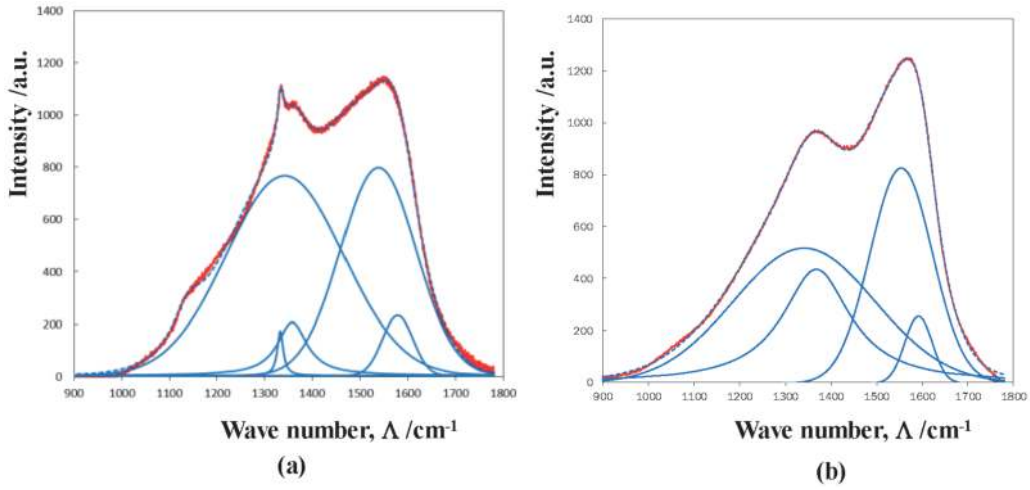

Figure 4.
Comparison of Raman spectra before and after the pulsed laser post-treatment. (a) Raman spectra before treatment, and (b) Raman spectra after treatment.

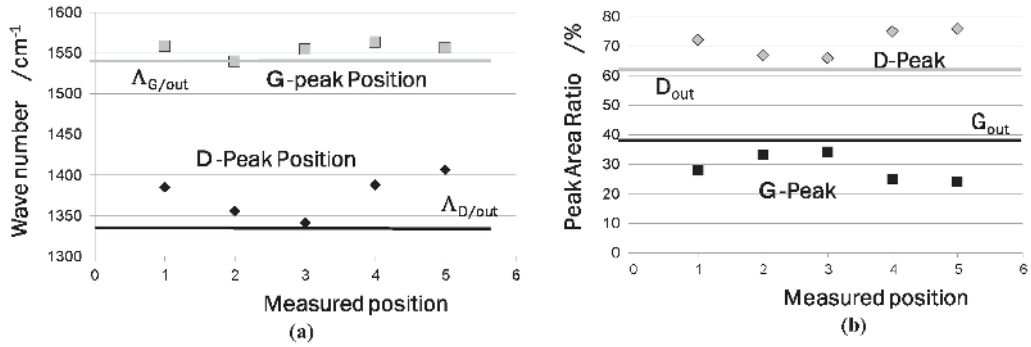

Figure 5.
Characterization on the laser-processed diamond coatings with comparison to unprocessed film. (a) Distribution of Λ_G and Λ_D on the micro-grooved surface with comparison to the average Λ_G and Λ_D outside of the microgrooves, and (b) distribution of peak area ratio for G- and D-peaks on the micro-grooved surface with comparison to the average peak area ratios outside of the microgrooves.

1340 cm^{-1}, the crystalline G peak at 1580 cm^{-1} and sp3 diamond peak at 1320 cm^{-1}. This reveals that CVD-coated diamond film consists of the nano-structured matrix of sp3 – sp2 binding-state carbon and the sp3-rich surface structure. After pulsed laser adjustment, this surface diamond D-peak disappears in **Figure 4b**. The same broad graphitic D and G peaks are deconvoluted from the measured spectra in **Figure 4a** and **b**. Remember that amorphous carbon films are also characterized by these D and G peak pair [10] and that carbon dusts are only detected by low intensity Raman spectra with much broadness [11]. Although the near-surface of diamond coating is affected by laser irradiation, its depth might be characterized by the diamond D-peak as well as these graphitic D and G peak pair [35]. No essential deterioration occurs in this sizing process of the diamond coating. The surface layer with characteristic sp3 nanostructure is only ablazed during irradiation.

The quality profile of processed diamond coating is investigated by analyzing these graphitic D- and G-peak distributions in the longitudinal direction of micro-groove. **Figure 5a** depicts the Raman shift distributions; the graphitic D-peak Raman shift increases to the higher wave number from the center to both ends. As shown in **Figure 5b**, the graphitic D-peak area ratio is nearly constant and higher than 65%. In particular, the measured D-peak area ratio at the micro-groove bottom

is always higher than that on the original diamond film. This also proves that the surface of sized diamond coating by the pulse laser irradiation has no significant deviation in quality of coating materials.

5. Femtosecond laser trimming of diamond-coated tools

Femtosecond laser irradiation system was utilized to trim the as-coated diamond film surfaces, to sharpen the punch edge and to make nanostructuring on the side surface of cylindrical punch. SEM with various magnifications was used to make microstructure analysis on these nanostructures. The white light interferometry was also employed to characterize them.

5.1 Trimming and nanostructuring

A CVD-diamond coated WC (Co) punch with the diameter of 2.00 mm was prepared for the present laser trimming and nanostructuring. As shown in **Figure 6a**, the original head and side surfaces of as-coated diamond film are rough by the polycrystalline diamond growth during CVD; e.g., its maximum surface roughness reaches to 5 μm. The punch edge curvature also becomes dull as an intersection of rough head and side surfaces.

Figure 6b shows the laser-trimmed punch profile after surface cleaning. The maximum roughness of punch head is reduced down to 0.5 μm on the measured surface profile. Both head and side surfaces are laser-trimmed so that the punch edge is considered to be sharpened as an intersection of two surfaces.

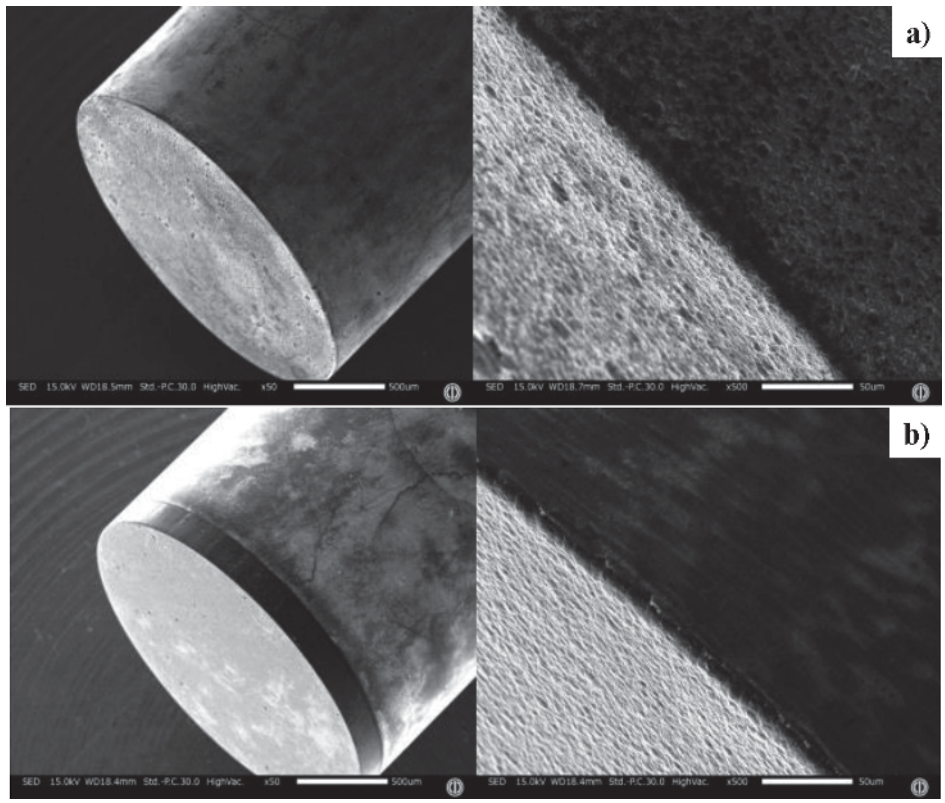

Figure 6.
Comparison of SEM image before and after laser treatment. (a) As-coated head and side surfaces with a dull edge, and (b) laser-trimmed head and side surfaces with a sharpened edge.

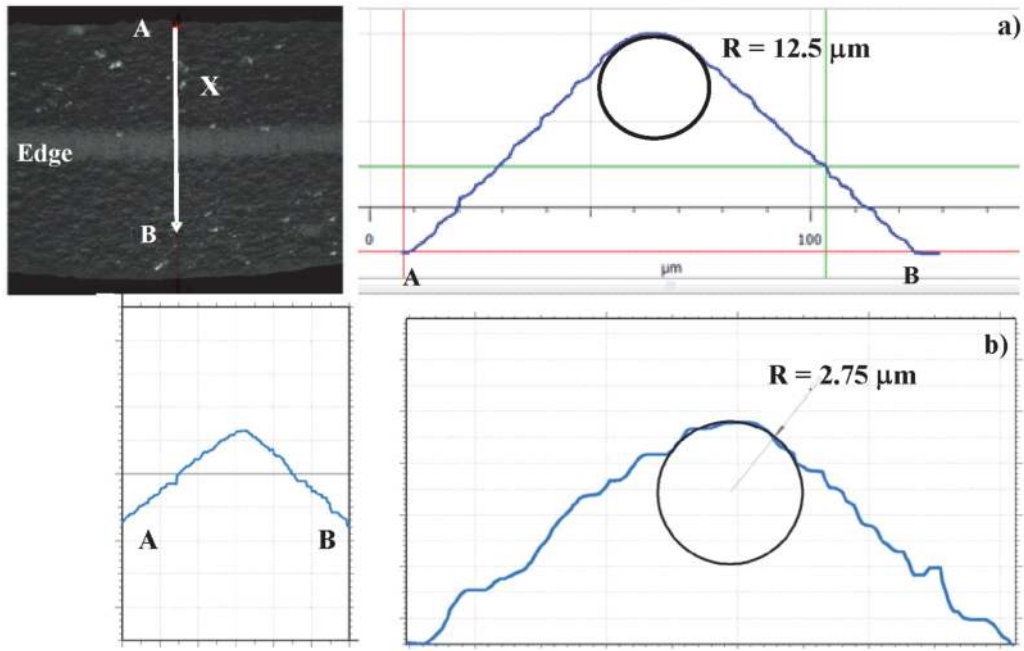

Figure 7.
Comparison of punch edge curvature before and after laser treatment. (a) before laser trimming, and (b) after laser trimming.

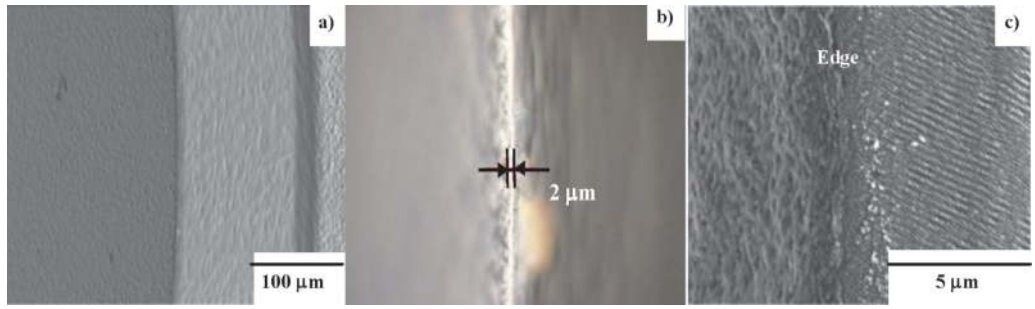

Figure 8.
SEM and LM images on the laser treated side surface from the punch edge. (a) SEM image on the laser-trimmed head and side surfaces of punch in low magnification, (b) LM image around the punch edge, and (c) SEM image across the punch edge in high magnification. A nanostructure was formed to have a regular alignment with its period of 300 nm.

Figure 7 compares the punch edge curvature radius before and after laser trimming. As-coated edge curvature radius (R) is 12.5 μm; this large R is reduced down to 2.75 μm by this trimming. This improvement proves that femtosecond laser trimming is effective to sharpen the punch edge width down to 2 μm.

5.2 Controllability of nanostructures

The femtosecond laser trimming process accompanies with nano-structuring on the trimmed surfaces. When laser-trimming the diamond coating, LIPSS takes place to form the intrinsic nano-textures with the LIPSS-period to the optical interaction between the laser beam scattered by the rough diamond surface and the incident laser beam. SEM was utilized to describe this simultaneous nano-structuring with trimming process in the above. **Figure 8a** shows the SEM image of head and side surfaces of punch. The punch edge width (W_E) is also measured by LM (Laser

Microscopy) in **Figure 8b**. W_E = 2 μm just in correspondence to R = 2.75 μm in **Figure 7b**. **Figure 8c** depicts the change of microstructure from the punch head to its side surface across its edge. The trimmed head surface changes to the nanostructured surface just across the edge. This nanostructure consists of the regularly aligned nano-grooves with the LIPSS period of 300 nm. This measured pitch is corresponding to the estimated LIPSS period of 250 nm when using the above femtosecond laser processing conditions.

White light interferometry (WLI) was utilized as a nondestructive evaluation method for diagnosis of nanotextures on the trimmed punch surface profile. This WLI is usually utilized to measure the geometric angulation of polished and buffed die surfaces with relatively little curvature radius. In this measurement, a trimmed diamond-coated punch with the diameter of 2.00 mm has a curvature with influence on the interferometric measurement on the spatial period of nanotextured ripples on the trimmed surface. **Figure 9a** shows this local surface profile in this X-axis or in the lateral direction of punch surface, which was analyzed by the algorism of DEAP (Detection of Envelope and Absolute Phase) [36]. This profile gradually deviates from the center line; the nanotextures are formed on the trimmed punch surface with the skewed angle in the axial direction. The measured spatial period of nanotextures (Λ_{punch}) is 900 nm, and, their average height reaches to 300 nm.

Let us consider the difference in the spatial period of nanostructures, between the measured Λ_{punch} of 900 nm in **Figure 9a** and the LIPSS-period of 300 nm in **Figure 8c**. In the detection of fine spatial peaks in the large area with the curvature by WLI, the neighboring peaks to a main peak are easily enveloped into a single signal by the DEAP algorism. Then, the WLI-measured period becomes three times more than the actual ripple period of 300 nm. In other words, the curvature effect to the measured profile of peaks cannot be sufficiently eliminated in the present measurement.

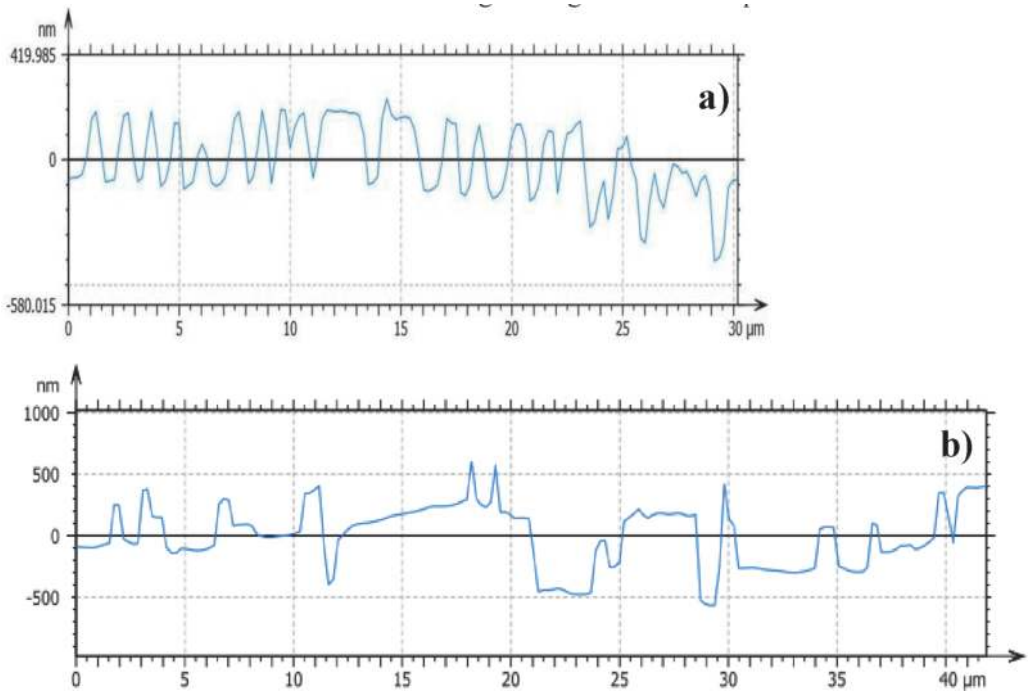

Figure 9.
White light interferometry of the nano-structured diamond-coated punch as well as the imprinted nanotextures onto the hole surface together with the piercing process of AISI316L sheets. (a) Nano-structure on the diamond coating, and (b) imprinted nanotextures on the pierced hole surface.

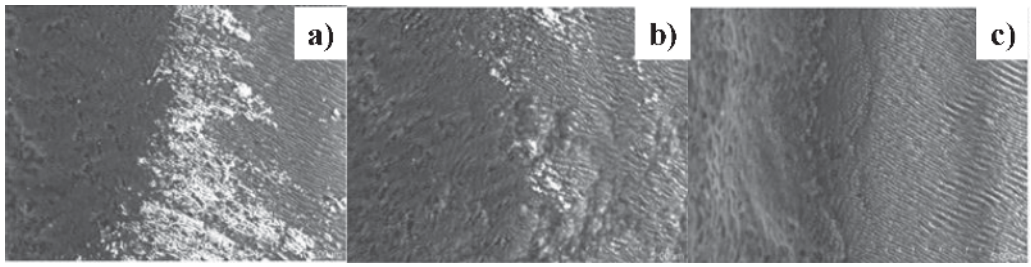

Figure 10.
Effect of the threading depth (d) in the laser trimming process on the nanostructures formed on the punch side surface. (a) d = 1.8 μm, (b) d = 2.4 μm, and (c) d = 3.6 μm.

In the present trimming of the diamond coating on the cylindrical punch, the scattering laser on the coating is skewed by the local curvature on the trimmed diamond surface so that every nanotextured ripple is formed in the axial direction with a skewed angle. This nanotexturing process with trimming the cylindrical diamond coating is mainly governed by this local curvature of cylindrical punch as well as the original roughness of diamond coating.

As pointed out in [33, 34], the laser processing parameters also have influence on this LIPSS or nanotexturing onto the laser-trimmed surface. Among them, the laser pulse width has a direct influence on the ripple-period while the fluence of laser beam affects the LIPSS-profile more than the LIPSS-period. In particular, the depth of nanostructure is incrementally increased by increasing the number of pulses or by increasing the fluence. This laser beam fluence was varied to investigate the effect of irradiation fluence on the depth of nanostructures. **Figure 10** compares the SEM images on the nanotextures on each trimmed surface among three punches. Although the peak-to-valley ratio of nanotextures increases with d, the unidirectional formation of nanotextures with a skewed angle is common to three punches. The measured LIPSS-period is also common to three cases; e.g., Λ_{punch} = 300 nm. The similar nanotexturing profile are simultaneously machined onto the diamond coating with trimming; its depth is mainly determined by the fluence.

6. Ultra-fine piercing of stainless steel sheets by laser-treated punch

AISI316L austenitic stainless steel sheets with the thickness of 0.2 mm were utilized for fine piercing experiments with the use of the treated CVD-coated WC (Co) punch. SEM and white light interferometry were also employed to characterize the quality of pierced products.

6.1 Fine piercing system

Figure 11a depicts a piercing experimental set up where the stroke is controllable in every 1 μm. The relationship between the piercing load and the punch stroke is monitored during this piercing process. The laser trimmed diamond-coated WC (Co) punch with a diameter of 2.000 mm was fixed into an upper die in the cassette die-set for the piercing experiment. The WC (Co) core die with an inner diameter of 2.008 mm was also placed into the lower die. The load cell was embedded into the lower die set to monitor the applied load in every stoke. As illustrated in **Figure 11b**, the narrow clearance between the punch and die is controlled by the nano-metric PZT X-Y stage to preserve the coaxial position of punch to die.

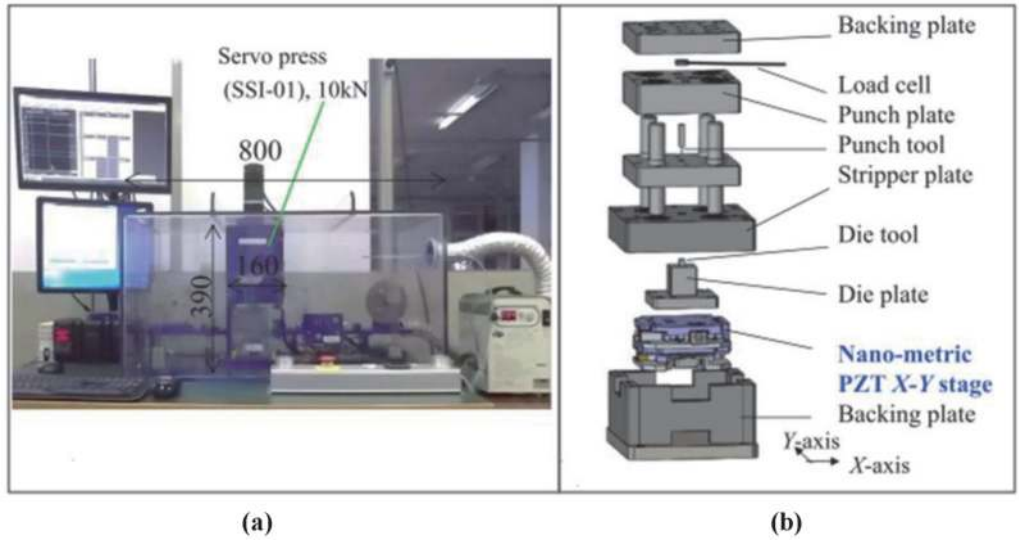

Figure 11.
Aluminum-flamed fine stamping system with high stiffness in the die set and flexible stamping structure. (a) Overview on the CNC mini-stamping with the maximum loading capacity of 10 kN, and (b) illustration of the die set.

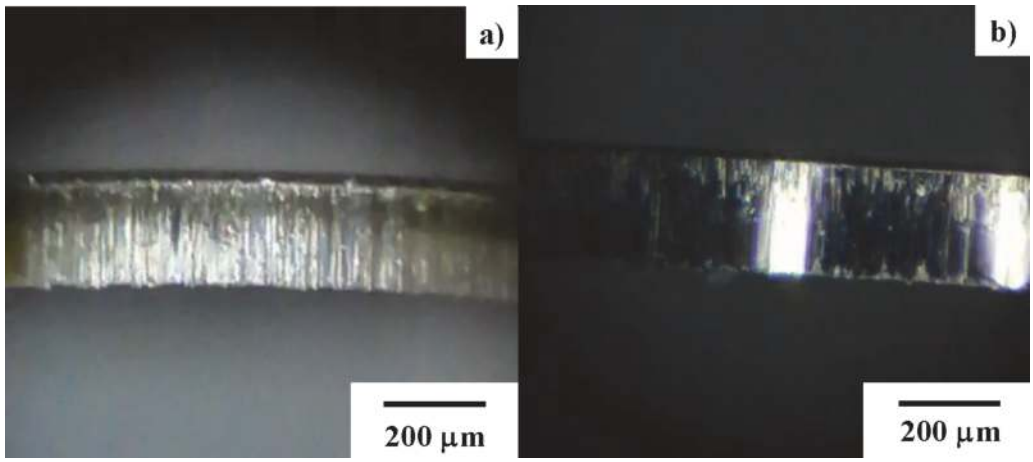

Figure 12.
Comparison of the optical-microscopic image on the pierced AISI316L hole surfaces when using two punches. The edge curvature in both punches is nearly the same as 2 μm. (a) Pierced hole surface by the normal WC (Co) punch with the sharpened edge, and (b) pierced hole surface by the laser-treated diamond-coated WC (Co) punch.

6.2 Product qualification

The WC (Co) punch with the sharpened edge was also used as a reference punch for comparison of pierced hole surface to the present approach. **Figure 12** compares the sheared surfaces by piercing process with the use of WC (Co) punch and trimmed diamond coated one after 100 shots in continuous.

As depicted in **Figure 12a**, AISI316L sheet was punch out with full burnished surface area ratio even when using the WC (Co) normal punch with the sharpened edge. This fully sheared surface had lots of scratches since the side surface roughness of WC (Co) punch was transcribed onto the hole surface during the piercing process. When using the trimmed diamond-coated punch, the pierced hole also has no fractured surfaces in **Figure 12b**. In addition, this surface has a mirror-shining surface condition with tiny scratches only on its top. The length of nanostructured side surface from the punch edge is 200 μm and equal to the sheet thickness.

Irregular texture between the nano-textured and non-textured side surfaces induced these scratch markings. The essential difference in the pierced surface condition comes from the shearing process by the punch with and without the nanotextures on its side surface from its edge.

Let us analyze the pierced hole surface condition by the nanostructured punch from the multi-dimensional view. As shown in **Figure 13**, SEM observation is made from the lowest magnification to the highest one. As seen in **Figure 13a** and **b**, the pierced surface looks smooth without any scratches just in correspondence to the optical-microscopic observation in **Figure 12b**. With increasing the magnification, this smooth surface is found to have nano-stripes as shown in **Figure 13c** to **13e**. This reveals that nanostructures with the period of 300 nm on the diamond coated punch are imprinted onto the pierced hole surface as nano-stripes. **Figure 13f** proves this imprinting of nanostructures to product surface together with piercing the AISI316L sheet.

WLI is also utilized to make nondestructive analysis on the imprinted nanotextures in **Figure 13f**. **Figure 9b** depicts the pierced hole surface profile. In correspondence to nano-stripes in **Figure 13f**, nano-textures are detected on the hole surface. The DEAP alogorism in WLI also biased the measurement of nanotextures on the pierced hole by its local curvature to provide Λ_{hole} = 900 nm in **Figure 9b**. Since $\Lambda_{punch} = \Lambda_{hole}$ = 900 nm by WLI in **Figure 9**, the nanostuctures on the punch side surface is simultaneously imprinted onto the hole surface together with piercing the hole.

In the algorithm of DEAP, the effects of large curvatures on the interferometric measurements are difficult to avoid when analyzing nanotextured periods on the punch and pierced hole surfaces. The nanotextures on the punch and hole surfaces were over-estimated to have larger periods by this curvature effect in the WLI and DEAP analysis.

6.3 Ejection of debris particles

The debris particles splash in the air, easily deposit on the die surfaces and often lock the further steps in cutting and piercing the work materials. In particular, when

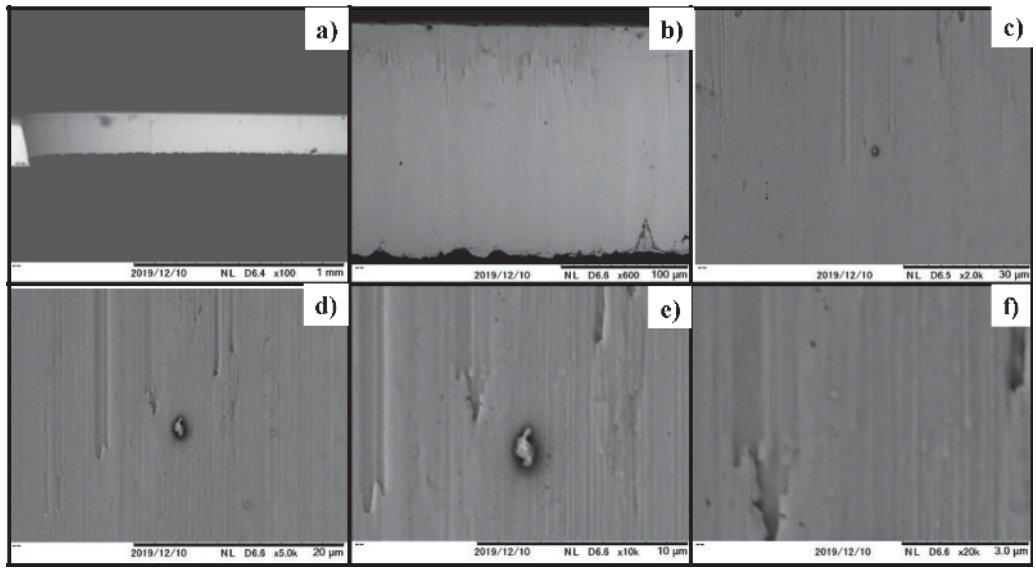

Figure 13.
SEM image on the pierced AISI316L hole surface by using the laser treated diamond-coated WC (Co) punch with varying the magnifications from (a) to (f).

fine piercing the work in the narrow clearance, they deposit on the punch head and side surfaces under high static pressure. This deposition increases the friction and wear in piercing, and damages to the tools. In the lubricated conditions, those particles are trapped into the lubricating oils and ejected to outside of cutting and stamping processes together with liquid lubricants. However, in the case of dry piercing of works, there are no ways to pocket the splashing particles and push out them from the piercing front on the interface between punch and work to its end. Those residual debris particles adhere to the punch surface and lock the piercing process at the risk of severe damage to punch edge and surfaces. Hence, how to trap those debris particles and to eject them out of the piercing system becomes an issue to promote the production quality in fine piercing.

The nanotextures formed on the punch side surface are expected to be working as a nano-groove to trap and eject these debris particles from the vicinity of punch edge to the length of punch. After continuously piercing the AISI316L sheets in a thousand shots, the punch surface was precisely analyzed by SEM. **Figure 14** depicts the punch head and side surfaces with varying the magnification in SEM observation. As seen in **Figure 14a**, no adhesion of debris particles is detected on both surfaces. With increasing the magnification in SEM, the iron-rich debris particles of AISI316L are trapped into the nano-grooves on the side surface as shown in **Figure 14b** and **c**. As depicted in **Figure 14c**, most of nano-grooves trap the debris away from the punch edge by 8 μm.

The nanotextures were formed from the punch edge to the length of 0.2 mm along the punch axis. Consider that this punch is pierced into the AISI316L sheet, and the sheared debris fragments by the sharp punch edge are infiltrated into these nanotextures. As seen in **Figure 14**, less amount of particles is trapped at the vicinity of punch edge but a lot of particles are lodged into them even far from the edge by 100 μm. This suggests that the trapped debris particles are transferred from the punch edge to the punch length during the piercing process. In order to demonstrate this transfer process, the whole punch surface is precisely analyzed along the length of punch. **Figure 15** depicts how the debris particles are trapped and transferred to the punch length (L).

As stated before, little debris fragments are trapped at the vicinity of the punch edge. They fill into the nanostructured grooves; e.g., at L = 8 μm from the edge, most of grooves are stacked by them. To be interested, they overlapped the groove and form an agglomerate of debris fragments at L = 15 μm. Each nano-groove first traps a debris fragment and is gradually packed by debris with increasing the number of shots in piercing. Once the amount of debris exceeds the trapping capacity to fully pack the fragments with the length of 2 μm for each nano-groove, the debris fragments agglomerate to a platelet. These platelets are only seen around L = 15 μm. Since no platelets were seen for L > 15 μm, they delaminate from nanostructured punch surface and transfer to further length of punch.

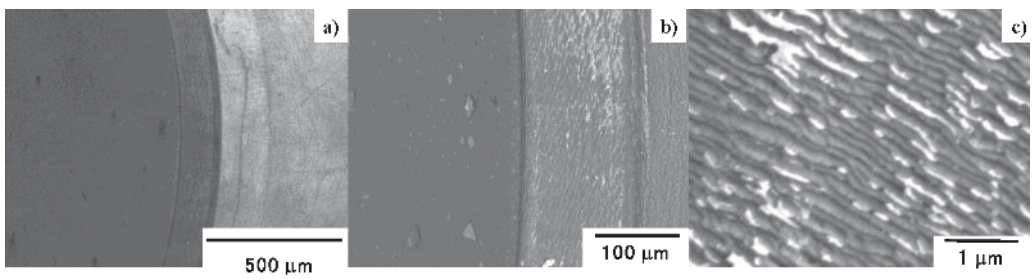

Figure 14.
SEM image on the laser-treated diamond-coated punch near the sharpened edge. (a) Lowest magnification, (b) lower magnification, and (c) higher magnification.

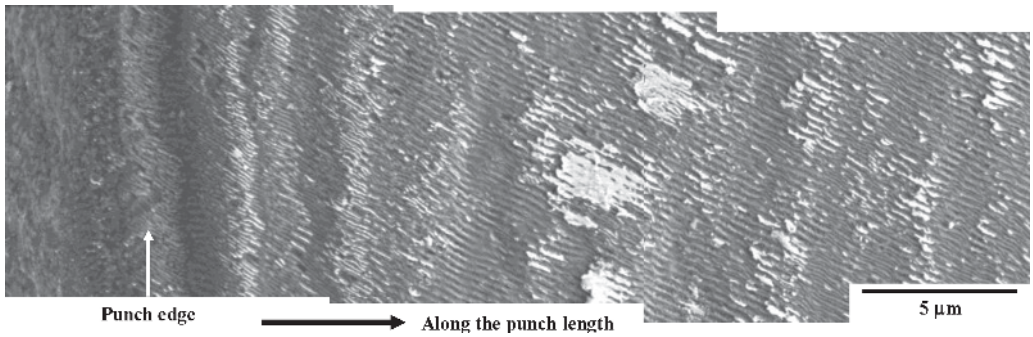

Figure 15.
Fine SEM image on the laser-treated diamond-coated punch from the sharpened punch edge to the end of post-treated zone.

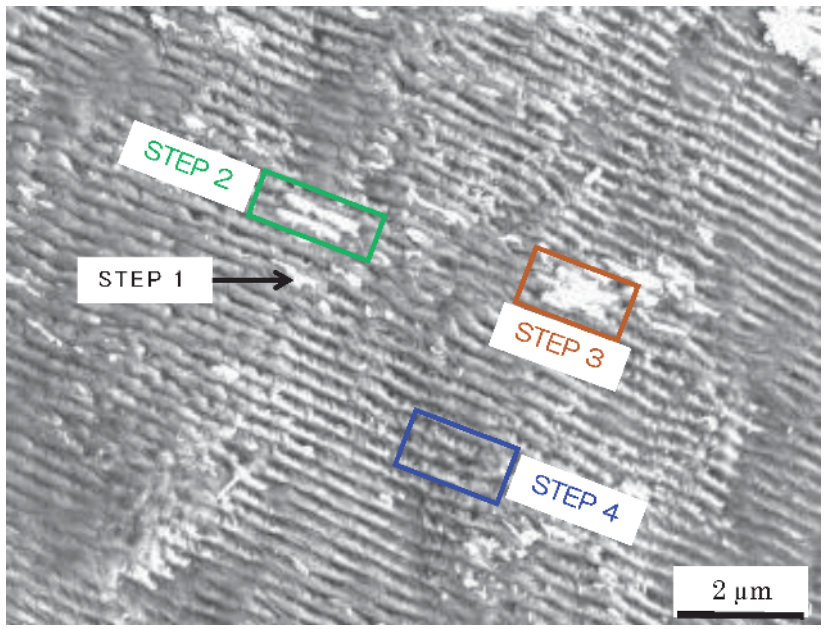

Figure 16.
Ejection model to capture, release and transfer the debris particles from the piercing front to the outside.

Let us consider this ejection mechanism of debris particles in dry piercing. Due to precise SEM analysis on the nano-textured punch surface after continuous piercing in 1000 shots, various steps in this mechanism are described as shown in **Figure 16**.

At the step-1, the AISI316L debris particles are trapped into a single nano-groove. This first trapping of debris occurs on the contact interface of nanostructured punch surface and AISI316L work under high static pressure during every shot in piercing. With increasing the number of shots, the probability also increases for the debris particles to be trapped into two adjacent nano-grooves in the setp-2. In further continuous piercing, each trapped debris agglomerates on a couple of nano-grooves in the step-3. When the size of agglomerates exceeds the critical volume of 5 μm^3, they delaminate by themselves and dislodge to be pushed down into the punch length during the shearing process in piercing. At the step-4, the nano-groove becomes vacant enough to trap new debris particles in further piercing process. This ejection mechanism of debris particles during the piercing is effective to be free from their locking to clearance and to continue the fine piercing process with high product quality.

7. Discussion

CVD-diamond, polycrystalline and single-crystal diamonds have intrinsic hardness ranging from 5000 HV to 10000 HV, controllable electric resistivity by doping from 100 GΩ·m to semi-conductivity, high thermal conductivities around 2200 W/(m·K), and high thermal stability. In its industrial applications to piercing punches and dies, their laser adjustment and surface treatment is indispensable to make full use of these properties.

The original roughness of bare diamond coating by its tetragonal crystal growth is in the order of 3 to 5 μm. As demonstrated in **Figure 3**, its maximum roughness can be lowered to be less than 0.8 μm even by the multi-pulse laser irradiation. A microgroove with the length of 10 mm, the width of 125 μm and the depth of 3.8 μm is accurately cut into the diamond film. This proves that the tailored geometry for fine piercing punch is shaped onto the diamond coating within the tolerance of submicron meter.

When using the femtosecond laser-treatment, the surface roughness is much reduced as shown in **Figure 6** through the laser beam control in **Figure 2b**. This suggests that the punch edge as an intersection of its head and side surfaces can be sharpened by trimming these two surfaces and reducing their surface roughness. **Figure 7** proves that the punch edge sharpening is driven by this surface trimming processes in **Figure 2b**. The most preferable merit to this femtosecond laser treatment is a simultaneous nano-structuring on the punch side surface together with the laser trimming process. As depicted in **Figure 8**, this nanostructuring by LIPSS commences just from the punch edge to the length on its side surface. The period of induced nanostructures is dependent on the laser pulse width, the fluence and the laser beam control in addition to the diamond film surface roughness. Their depth into the diamond is mainly controlled by the fluence in laser trimming, as shown in **Figure 10**. The direction of nanostructures is also tunable by the optical control.

In addition to the skew angled nanostructures in **Figures 8c** and **10**, each nanostructure by LIPSS can be formed in the circumferential and longitudinal directions,

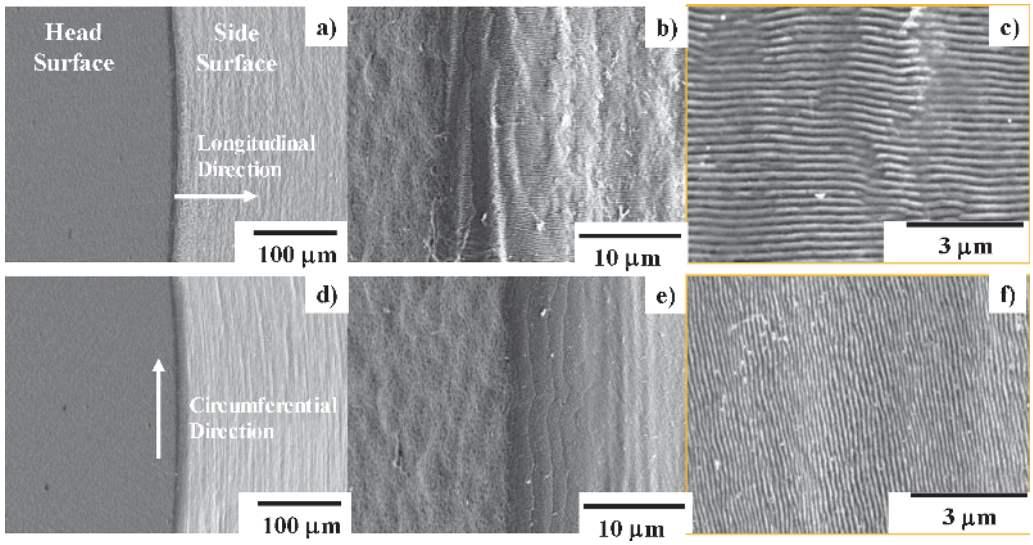

Figure 17.
Controllability of the laser-induced nanostructures onto the side surface of CVD diamond-coated punches. (a-c) A longitudinal alignment of nanostructures on the trimmed punch with varying the magnification in SEM, and (d-f) a circumferential alignment of nanostructures on the trimmed punch with varying the magnification in SEM.

respectively, by the polarization technique [37]. **Figure 17** depicts two typical nanostructure alignments onto the diamond-coated punch side surface. SEM images in **Figure 17a** to **17c** with varying the magnification, depict the longitudinally aligned nano-grooves along the punch length. **Figure 17d** to **17f** show the SEM images on the circumferentially aligned nano-grooves with varying the magnification. The direction of nanostructures as well as their LIPSS periods are modified by this polarization control. In particular, when controlling the formation of nanogrooves in the circumferential direction, the LIPSS-ripples have smaller period of 100 nm than 300 nm for the nanogrooves formed in the longitudinal direction.

This control of nanogroove directions has direct influence on the piercing behavior. As introduced in [38], the sharpened punch edge behaves as a blade to cut into the work at the beginning of the piercing process as illustrated in **Figure 18**. The droop is formed by elastoplastic deformation of work at the indentation of punch, and the sheared work surface is generated by the contact of work to punch side surface before final fracture. In the nanostructured punches, each LIPSS-formed nanostructure works as a blade to advance the shearing process in piercing.

When using the nanostructured punch in **Figure 17a** to **17c**, the straight nano-grooves are imprinted onto the pierced hole surface to have the LIPSS-period of 300 nm. During this piercing process, the debris fragments are easily driven to the length of punch. On the other hand, when using the nanostructured punch in **Figure 17d** to **17f**, the finer nano-grooves with the LIPSS period of 100 nm are formed in the circumferential directions on the pierced hole surface. Every debris particle is stacked in each nano-groove during piercing. These ejection processes with dependence on the nanostructure alignment have an importance role to preserve the high quality piercing of work and prolong the punch life without damages by debris particles.

Let us reconsider the effect of debris particle fragmentation to the piercing process. How to deal with the debris particles is an essential issue in mechanical machining and metal forming. As proposed in [22, 39, 40], the micro-dimples on the rake surface of cutting tools work as a micro-reservoir to stock the debris particles. In case of end-milling of aluminum alloys, the machined chips stack to

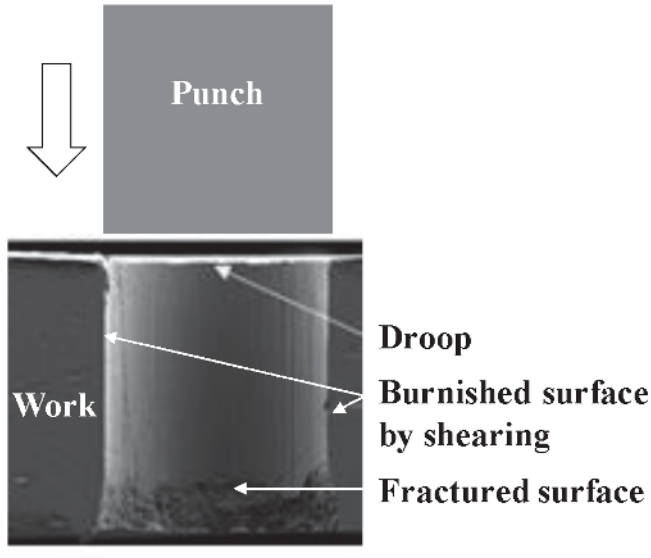

Figure 18.
Schematic view on the cross-section of pierced hole in the AISI316L work by punching. A droop was formed by the initial indentation of punch; then, the burnished and fracture surfaces are formed by this shearing process of ductile work.

these dimples so that the adhesion wear of debris to cutting tools is saved to prolong the cutting tool life. In the metal forming under lubricating oils, the debris particles are included into these lubricating oils and ejected together to outside of forming system. When using this micro-dimple technique, a lubricating oil is indispensable to house and drive the debris particles into the micro-dimples. In case of the dry machining and metal forming, how to trap and eject them out of the working space becomes an issue to prevent the tools and dies from severe damage and to be free from the shortage of their lives. Nano-structuring to cutting and metal forming tools proves a method for trapping and ejecting the debris fragments to outside of the cutting and forming systems together with the movement of tools.

How to preserve the product quality, becomes another issue to be solved by tooling appropriately. Although this problem is not so severe in cutting and machining, a product quality assurance during the metal forming is an essential issue for die and punch design. The product surface quality in piercing depends on the shearing process on the interface between punch surface and work and on the flow stress of work materials. During the piercing process, the initial contact interface starts at the punch edge; the strain concentration at the sharp edge drives the shearing process of work materials. Let us consider how the punch edge profile in the edge width influences on the piercing process.

Two types of punch are prepared for piercing the amorphous electrical steel sheets with the thickness of 25 μm. As shown in **Figure 19**, one is a WC (Co) punch with the sharpened edge width of 2 μm and another is a laser-trimmed diamond-coated punch also with the edge width of 2 μm. The difference in the geometric topology between two punch edges is noticed as an edge profile morphology. The WC (Co) punch has a diffusing edge profile as seen in **Figure 18a** to **18c** while the laser trimmed diamond-coated punch has a homogenous edge profile as shown in **Figure 18d** to **18f**. A brittle amorphous electrical steel sheet is employed to describe the effect of two edge profiles to its piercing behavior.

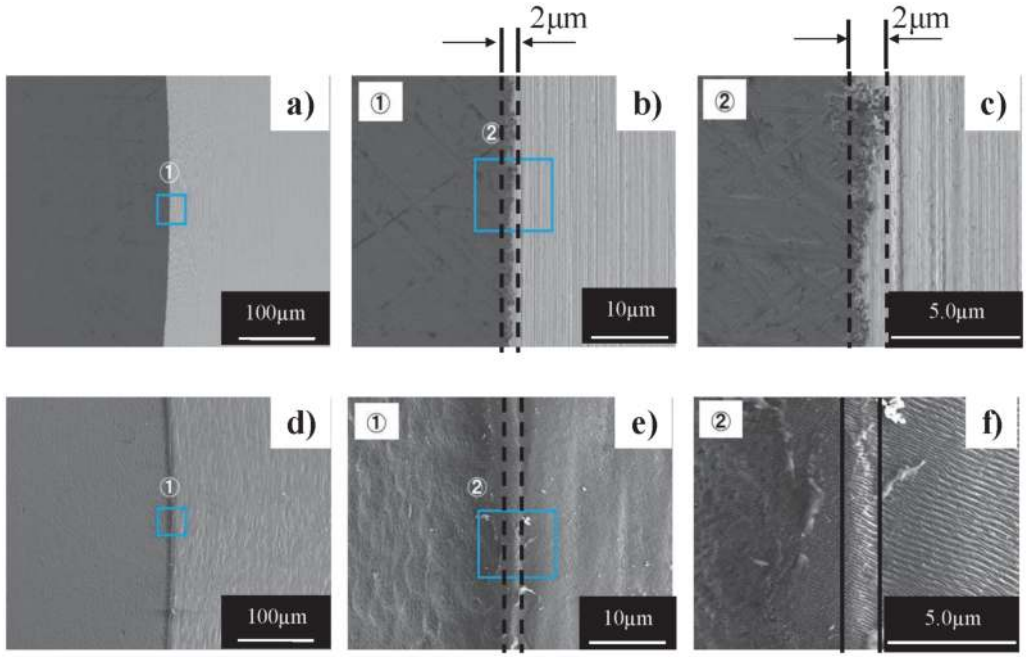

Figure 19.
Comparison of SEM images with different magnifications between two fine piercing punches with the same edge width of 2 mm . (a–c) WC (Co) punch with the sharpened edge width of 2 mm, and (d–f) diamond coated WC (Co) punch with the laser trimmed edge width of 2 mm.

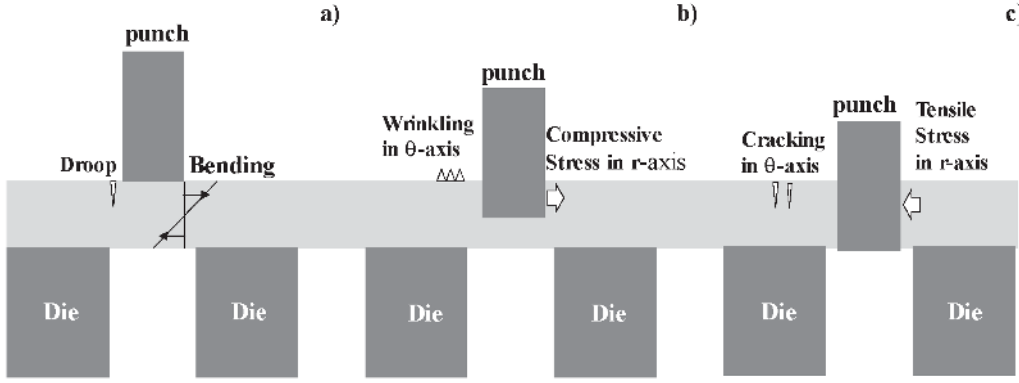

Figure 20.
Damaging process induced into the work sheet by the piercing process from (a) to (c). (a) Formation of a droop with circumferential cracks, generated by the initial indentation of punch to work, (b) formation of circumferential wrinkles, induced by the compressive stress in the radial direction, and (c) formation of circumferential cracks by perforation of a hole.

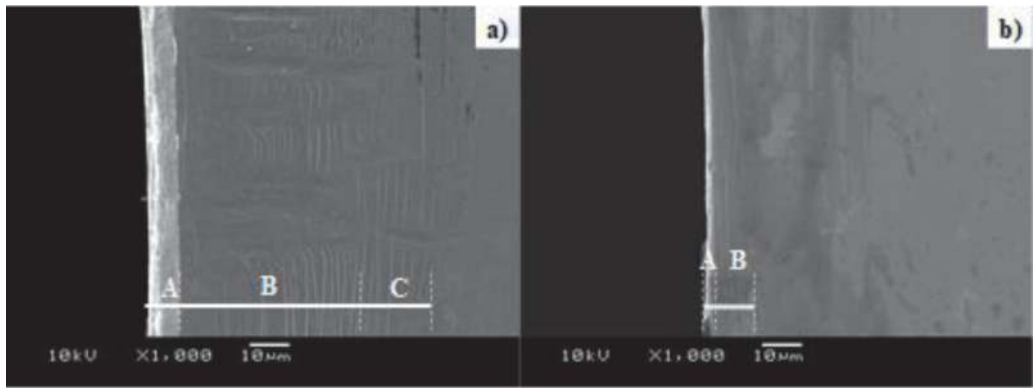

Figure 21.
Micro-damages induced into the amorphous electrical steel sheet by the piercing process. A-zone is a droop with the circumferential cracks at the stage of punch indentation. B-zone is a wrinkle with peaks and valleys where the short surface cracks are seen on the peaks. C-zone includes the long surface cracks in the circumferential direction. (a) When using the WC (Co) punch, and (b) when using the diamond-coated punch.

First in the punching process as depicted in **Figure 20**, a brittle material begins to make elastic shear deformation by initial indentation of a punch edge into it. This bending deformation by indentation of the punch edge, results in the formation of droop with surface cracks in the circumferential direction or in θ-axis. In further indentation of punch, the compressive stress is induced in the radial direction to push back the work material in shearing. Under this compressive stress state, the wrinkling occurs in θ-axis. When punching out, the tensile stress is applied to the work so that the circumferential cracks are generated in the work surface.

Figure 21 compares the pierced hole surface by two punches with the different edge profile. When using the sharpened WC (Co) punch, the droop, the wrinkling, and the circumferential cracking are all seen on the pierced sheet surface as A-zone, B-zone and C-zone, respectively in **Figure 21a**. On the other hand, the droop and the circumferential cracking are measured in **Figure 21b** when using the nano-structured diamond-coated punch. No circumferential wrinkling takes place in the latter. In addition, the circumferential cracking only occurs at the vicinity of hole surface. This difference does not come from the sharp edge width but from the homogeneous edge profile. As seen in **Figure 19**, the edge profile of sharpened WC (Co) punch is diffusing so that the circumferential distortion could be easily

induced by the compressive stress at the contact of convex punch edge parts to the work. In the case of the nanostructured punch with homogeneous edge profile, the brittle work sheet is sheared without the wrinkling in the circumferential direction. This difference in the piercing behavior suggests that nano-structured punch has possibility to reduce the induced defects by controlling the structure of nano-grooves such as the direction of nanostructures and their LIPSS-period and depth. The direction of nanogrooves is optimized to reduce the cracking damage; e.g., the longitudinal nanostructuring is recommended to reduce the A- and C-damage widths and to eject the generated debris fragments. The nanostructure depth of 3 to 5 μm is necessary to stimulate the plastic flow of ductile work around the edge profile and to improve the punch life. The LIPSS-period is designed to reduce the A-damage width as well as the piercing stress.

Let us be back to how to imprint the nanostructures by stamping as shown **Figure 11**. In case of the piercing process, the pierced hole surface is macroscopically smooth with metallic shining and microscopically has nanotextures on it. In case of the embossing and coining processes, the tailored nanotextured surfaces are directly imprinted onto various mechanical parts and tools. Nontraditional design on the micro−/nano-textures leads to development of new mechanical elements in application.

In fine piercing operations, most of piercing punches and dies have complex shaped heads and core-cavities with the accurate dimension, respectively. Let us evaluate on the application of the present laser trimming method to fabricate those complex-shaped punches and dies. A cross-lettered WC (Co) punch was employed for femtosecond laser trimming, as shown in **Figure 22a**. The laser-machining path schedule was optimized to make homogeneous machining the whole punch side surfaces around the cross-lettered head. **Figure 22b** shows the SEM image on the vicinity of punch edge with high magnification. The side surface was trimmed and nanostructured to have the LIPSS-period of 300 nm in the similar skewed angle as seen in **Figure 8c**. This demonstrates that the complexed shaped punches and dies are laser-trimmed to sharpen their edges and to form the nano-structures on their surfaces by the present laser-treatment.

In addition to the CVD diamond coatings, this simultaneous laser trimming with nanostructuring is successfully applied to the ceramic coated dies such as CrN, AlCrN and DLC as well as the nitrided and carburized tools. Those nanostructured

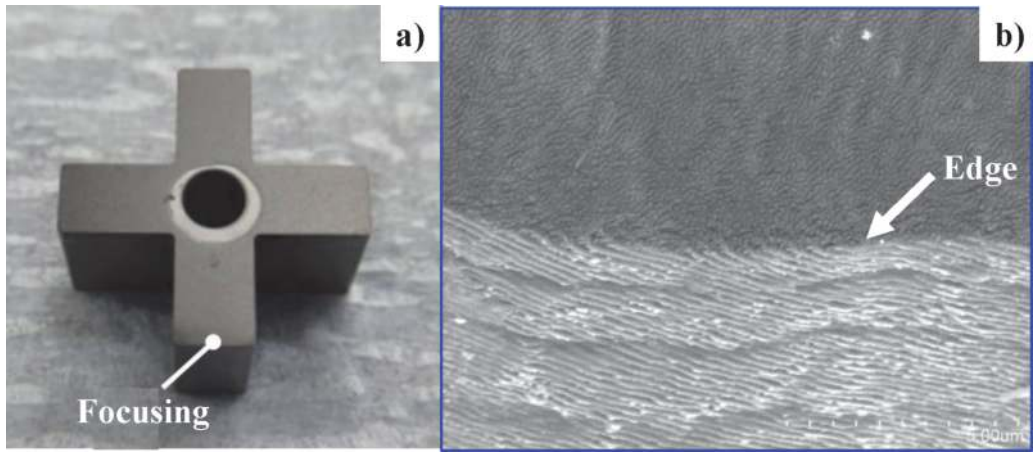

Figure 22.
Laser trimming of the complex shaped, diamond-coated WC (Co) punch for fine piercing. (a) Overview of the cross-lettered punch, and (b) nanostructured side surface of punch across its edge. The nanotextures are wavy in nature.

dies and tools work in metal forming to accurately yield the engineered surfaces onto the metallic products with higher cost-performance.

8. Conclusion

A circular economy stands on the sustainable manufacturing with high material efficiency, less emission of wastes and long-life tooling. The CVD diamond coated WC (Co) tooling grows up as a reliable method. The used diamond film was perfectly ashed with less damage to WC (Co) substrate. The tailored WC (Co) substrate is recycled as a tool after recoating the diamond films. Through the laser-treatment of recoated diamond layer, high qualification of products is put into practice together with prolongation of tool life. The laser-treatment provides a reliable method to resize the rough shape of as-coated diamond film into tailored geometry for punch and die in metal forming. No significant damages are generated through this processing. In particular, the femtosecond laser-treatment plays a role to adjust the as-coated diamond punch as a tool for ultra-fine piercing of stainless steel and amorphous electrical steel sheets at first. In second, the nano-textured surfaces are accommodated to punches and dies. In third, the laser-trimmed punch and die lives are prolonged with sufficient cost-competitiveness.

This laser treatment is characterized by the simultaneous edge-sharpening with nanostructuring. Especially, the laser-trimmed punch has a homogeneously sharpened edge with its width less than 2 μm. It has also a nano-structured side surface with the tailored LIPSS-period. In the fine piercing process, this nanostructure plays a double role. The pierced hole surface quality is improved from a fine surface with fully burnished area ratio to the hole surface to an ultrafine surface with mirror-polished condition. The generated debris fragments are ejected from the piercing front to the length of punch through this nanostructured groove. The affected zone width by piercing the ductile work is reduced by tailoring this nanostructures on the piercing punch. Since this zone of work experiences the plastic straining and strain recovery from plastic to elastic states, the reduction of its width improves the quality of products. In case of Fe-Si alloyed electrical steels, this reduction decreases the iron loss in the motor core and increases the product reliability as connector and sensing devices. In the similar manner, the damaged zone width of brittle amorphous sheets is also much reduced by this ultrafine piercing to lower the iron loss.

The imprinting method of nanostructures onto the product surface can be widely utilized to prepare for the engineered surfaces onto various products in application. Nanoscopic angulation onto the micro-textured product surfaces is useful to modify the original hydrophilic metallic surface to super-hydrophobic one. The critical heat flux of heat sink is enhanced by controlling the bubble nucleation at the imprinted micro-/nano-structure surfaces. The regularly aligned micro-/nano-structures surface work as an anti-bacteria part to prevent the human handling from infection. The tailored micro-/nano- textures on the medical tools assist a doctor to pick up and hold the targeting cells and organic parts. Through the imprinting process to dies and tools, various engineered surfaces are tailored and yielded onto the products.

Acknowledgements

The authors would like to express their gratitude to Mr. Y. Kira and Mr. S. Ishiguro (Graduate School of Engineering, University of Toyama) for their help in analysis. This study was financially supported in part by METI-program on the supporting industry, 2020.

Conflict of interest

The authors declare no conflict of interest.

Author details

Tatsuhiko Aizawa[1*], Tadahiko Inonara[2], Tomoaki Yoshino[3], Tomomi Shiratori[4] and Yohei Suzuki[3]

1 Surface Engineering Design Laboratory, SIT, Tokyo, Japan

2 LPS-Works, Co., Ltd., Japan

3 Komatsuseiki Kosakusho Co., Ltd., Japan

4 University of Toyama, Japan

*Address all correspondence to: taizawa@sic.shibaura-it.ac.jp

References

[1] Reineck I., Sjoestrand M. E., Karner J., Pedrazzini M., Diamond coated cutting tools. Int. J. Refractory Metals Hard Metals 14; 1996: 187–193.

[2] Konstanty J., Sintered diamond tools: trends, challenges and prospects. Powder Metallrugy 56(3); 2013: 184–188.

[3] Kuo C., Wang C., Ko S., Wear behavior of CVD diamond-coated tools in the drilling of woven CFRP composites. Wear 398; 2018: 1–12.

[4] Koga N., Usu K., Xu C., Deep drawing of thin stainless steel sheets using diamond tools without lubricant. J. JSTP 53; 2012: 74–78.

[5] Zhao G., Li Z., Hu M., Li K., He N., Jamil M., Fabrication and performance of CVD diamond cutting tool in micro milling of oxygen-free copper. Diamond and Related Materials 100; 2019: 107589.

[6] Aizawa T, Masaki E, Morimoto E, Sugita Y. Recycling of DLC-coated tools for dry machining of aluminium alloys via oxygen plasma ashing. Mechanical Engineering Research. 2014; 4(1): 52–62.

[7] Aizawa T, Sugita Y. High-density plasma technology for etching and ashing of carbon materials. Research Reports SIT. 2011; 55(2): 13–22.

[8] Aizawa T, Masaki E, Sugita Y. Oxygen plasma ashing of used DLC coating for reuse of milling and cutting tools. In: Proc. Int. Conf. Mater; Advanced Process Technology; 2011: 15–20.

[9] Aizawa T, Fukuda T. Micro-texturing onto carbon-based coatings via oxygen plasma etching. Research Reports SIT. 2012; 56(2): 66–73.

[10] Aizawa T, Fukuda T. Oxygen plasma etching of diamond-like carbon coated mold-die for micro-texturing. Surf. Coat. Technol. 2013; 215: 364–368.

[11] Aizawa T, Masaki E, Sugita Y. Complete ashing of used DLC coating for reuse of the end-milling tools. Manufacturing Letters. 2014; 2: 1–3.

[12] Aizawa T., Micro-manufacturing by controlled technologies. J. Automotive Engineering. 2018; 72 (6): 35–41.

[13] Aizawa T., Controlled post-treatment of thick CVD-diamond coatings by high-density plasma oxidation. In Ch. 4; Chemical Vapor Deposition for Nanotechnology, Intech Open 2019: 75–94.

[14] Yamauchi K., Aizawa A. High density plasma ashing of used diamond coated short-shank tools without damage to WC (Co) teeth. Proc. 11th ICOMM 2016; 50: 1–5.

[15] Yunata E. E., Aizawa T., Yamauchi K. High density oxygen plasma ashing of CVD-diamond coating with minimum damage to WC (Co) tool substrates. Mechanical Engineering. JSME 2016; CD-ROM.

[16] Yunata E. E., Aizawa T., Micro-grooving into thick CVD diamond films via hollow cathode. Manufacturing Letters. 2016; 4: 17–22.

[17] Roy S., Das M., Malik A.K., Balla V. K., Laser melting of titanium – diamond composites: Microstructure and mechanical behavior study. Mater. Lett. 2016; 178: 284–287.

[18] Popovich A. F., Ralchenko V. G., Balla V. K., Malik A. K., Khomich A. A., Growth of 4″ diameter polycrystalline diamond wafers with high thermal conductivity by 915 MHz microwave

plasma chemical vapor deposition. Plasma Sci. Technol. 2017; 19 (3): 035503.

[19] Dowson D., Dalmaz G., Childs T.H. C., Taylor C. M., Godet M., Wear Particles: From the Cradle to the grave. 1st Ed. 1992 Elsevier.

[20] Kirk A. M., Shipway P. H., Sun W., Bennett C. J., Debris development in fretting contacts - debris particles and debris beds. Tribology International. 2020; 149: 105592.

[21] Aizawa T., Satoh T., Shiratori T., Micro-joining of shaped stainless steel sheets for fuel injection orifice with high misting capability. Proc. 22nd Int. ESAFORM Conf. Mater. Form. AIP Conf. Proc. 2019; 2113: 050007–1.

[22] Aizawa T., Inohara T., Wasa K., Femtosecond laser micro−/nano-texturing of stainless steels for surface property control. J. Micromachines, MDPI 2019; 10–512: 2019: 1–12.

[23] Aizawa T., Wasa K., Tamagaki H., A DLC-punch array to fabricate the micro-textured aluminum sheet for boiling heat transfer control. J. Micromachines, MDPI 2018; 9–147: 1–10

[24] Aizawa T., Ono N., Boiling heat transfer control by micro−/nano-texturing of metallic heat-spreading devices. Proc. WCMNM2021 (in press).

[25] Shiratori T., Yoshino T., Suzuki Y., Nakano S., Yang M., Effects of ion processing of cutting edge of tools on tool wear and punching characteristics in mciropunching process. J. JSTP 2019; 60–698: 58–63.

[26] Enomoto Y., Soma K., Development of the amorphous motor balancing both resource saving and energy saving. J. Soc. Mech. Eng. 2014; 117: 753–756.

[27] Aizawa T., Inohara T., Multi-dimensional micro-patterning onto ceramics by picosecond laser machining. Res. Rep. Shibaura Institute of Technology 2012; 56 (1): 17–26.

[28] Aizawa T., Inohara T., Geometric adjustment and sizing of CVD-diamond coatings via oxygen plasma etching and laser machining. Proc. 7th SEATUC Conference (Bandon, Indonesia) 2013: 141–146.

[29] Aizawa T., Inohara T., Pico- and femtosecond laser micromachining for surface texturing. In Chapter 3 of Micromachining, InTechOpen, London, UK 2019: 35–62.

[30] Aizawa T., Shiratori T., Inohara T., Short-pulse laser precise trimming of CVD-diamond coated punch for fine piercing. Proc. 2nd Asian Pacific Symposium on Technology of Plasticity (APSTP) 2019: 123–128.

[31] Aizawa T., Shiratori T., Yoshino T., Inohara T., Femtosecond laser trimming of CVD-diamond coated punch for fine embossing. Mater. Trans. 2020; 61 (2): 244–250.

[32] Aizawa T., Shiratori T., Kira Yoshihiro, Inohara T., Simultaneous nano-texturing onto a CVD-diamond coated piercing punch with femtosecond laser trimming. Appl. Sci., MDPI 2020; 10, 2674: 1–12.

[33] van Driel H.M., Sipe J.E., Young J.F., Laser-induced periodic surface structure on solids: A universal phenomenon. Phys. Rev. Lett. 1982;49: 1955–1958.

[34] Aizawa T., Inohara T., Wasa K., Fabrication of super-hydrophobic stainless steel nozzles by femtosecond laser micro−/nano-texturing. Int. J. Automation Technol. 2020; 14 (2): 159–166.

[35] Prawer S., Nemanich R. J., Raman spectroscopy of diamond and doped diamond. Phil. Trans. Royal Soc. A

Mathematical Physical and Engineering Sciences. 2004; 362(1824): 2537–2565.

[36] Larkin K. G., Efficient nonlinear algorithm for envelope detection in white light interferometry. J. Opt. SoC. Am. 1996; 13 (4): 832–843.

[37] Tsubakimoto K., Miyaji G., Sueda K., Miyanaga N., Application of wavefront and polarization technique for power laser. Jpn. J. Optics. 2006; 35 (12): 635–642.

[38] Kira Y., Aizawa T., Suzuki Y, Shiratori T., Effect of punch edge profile to the piercing behavior of electrical amorphous steel sheet stacks. Proc. Autumnal Meting of JSTP 2020: 171–172.

[39] Sugihara, T., Enomoto, T., Performance of cutting tools with dimple textured surfaces: comparative study of different texture patterns. J. Int. Soc. Precision Engineering Nanotechnology. 2017: 49; 52–60.

[40] Aizawa, T., Morita, H., Tribological design and engineering in surface treatment for semi-dry and dry stamping. Proc. ICTMP2016. 2016: 14–28.